Electronic Supplementary Material (ESI) for Molecular BioSystems

Supplementary Material for: Inferring differences in the distribution of reaction rates across conditions

Diana M. Hendrickx [*†‡] Huub C.J. Hoefsloot [§*‡] Margriet M.W.B. Hendriks [†‡]
Daniël J. Vis [*†‡] André B. Canelas [¶‖] Bas Teusink[‖] Age K. Smilde[*‡]

[*]Biosystems Data Analysis, Swammerdam Institute for Life Sciences, University of Amsterdam, The Netherlands
[†]Department of Metabolic Diseases, University Medical Centre, Utrecht, The Netherlands
[‡]Netherlands Metabolomics Centre, Leiden, The Netherlands
[§]email: H.C.J.Hoefsloot@uva.nl
[¶]Kluyver Centre for Genomics of Industrial Fermentation, Biotechnology Department, Delft University of Technology, The Netherlands
[‖]Systems Bioinformatics, Centre for Integrative Bioinformatics, Free University of Amsterdam

1 Results of the simulations with the hypothetical networks

1.1 Glycolysis

Supplementary Table 1: Results obtained by changing one parameter in the hypothetical network in Figure 6. Two simulations were performed for each parameter: one by increasing, the other by decreasing it. Results in accordance with the experimental data are indicated in red. Abbreviations: see Figure 6 of the main text.

	G6P/F6P **A**	**FBP** **B**	**GAP/DHAP** **C**	**BPG/3PG** **D**	**GLYC** **E**	**In accordance with experimental data?**
experimental data - aerobic conditions	↗	↗	not measured	↘	not measured	
k_1 ↗	constant	↗	↗	↗	↗	no
k_1 ↘	↗	↘	↘	constant	constant	no
k_2 ↗	↗	↘	↗	↗	↗	no
k_2 ↘	↗	↗	↘	↘	↘	yes
k_3 ↗	↗	↗	↗	↘	↘	yes
k_3 ↘	↗	↗	↗	↗	↘	no
k_4 ↗	↗	↗	↘	↗	↘	no
k_4 ↘	↗	↗	↗	↘	↗	yes
k_5 ↗	↗	↗	↗	↗	↘	no
k_5 ↘	↗	↗	↗	↗	↗	no
k_6 ↗	↗	↗	↗	↘	↗	yes
k_6 ↘	↗	↗	↗	↗	↗	no

1.2 TCA cycle

Supplementary Table 2: Results obtained by changing one parameter or the behavior (cycle → 2 branches) in the hypothetical network in Figure 9, when the pathway acts as a cycle before the pulse (aerobic respiration). Two simulations were performed for each parameter: one by increasing, the other by decreasing it. Results in accordance with the experimental data are indicated in red. Abbreviations: see Figure 9 of the main text.

	PYR **A**	**ETH** **B**	**MAL** **OAA** **C**	**CIT** **ISOCIT** **D**	**FUM** **E**	**OGL** **F**	**SUC** **G**	**In accordance with experimental data?**
data aerobic	↗	not measured	↗	↘	↗	↗	↗	
k_1 ↗	↗	↗	↗	↗	↗	↗	↗	no
k_1 ↘	↗	↗	↘	↘	↘	↗	↘	no
k_2 ↗	↗	↗	↗	↘	↗	↗	↗	yes
k_2 ↘	↗	↗	↘	↗	↘	↘	↘	no
k_3 ↗	↗	↗	↗	↗	↗	↘	↗	no
k_3 ↘	↗	↗	↘	↗	↘	↗	↘	no
k_{4a} ↗	↗	↗	↗	↗	↗	↗	↘	no
k_{4a} ↘	↗	↗	↘	↗	↘	↗	↗	no
k_{5a} ↗	↗	↗	↗	↗	↘	↗	↗	no
k_{5a} ↘	↗	↗	↘	↗	↗	↗	↗	no
k_6 ↗	↗	↗	↘	↗	↗	↗	↗	no
k_6 ↘	↗	↗	↗	↗	↗	↗	↗	no
k_8 ↗	↗	↗	↗	↗	↗	↗	↗	no
k_8 ↘	↗	↘	↗	↗	↗	↗	↗	no
k_9 ↗	↗	↘	↗	↗	↗	↗	↗	no
k_9 ↘	↗	↗	↗	↗	↗	↗	↗	no
k_{10} ↗	↗	↗	↘	↗	↘	↗	↘	no
k_{10} ↘	↗	↗	↗	↗	↗	↗	↗	no
k_{11} ↗	↗	↗	↘	↗	↘	↘	↘	no
k_{11} ↘	↗	↗	↗	↗	↗	↗	↗	no
2 branches	↗	↗	↗	↘	↗	↗	↗	yes

Supplementary Table 3: Results obtained by changing one parameter in the hypothetical network in Figure 9, when the pathway acts as two branches (fermentation). Two simulations were performed for each parameter: one by increasing, the other by decreasing it. The scenario which qualitative behavior is most similar to the experimental data is indicated in red. Abbreviations: see Figure 9 of the main text.

	PYR **A**	**ETH** **B**	**MAL** **OAA** **C**	**CIT** **ISOCIT** **D**	**FUM** **E**	**OGL** **F**	**SUC** **G**	**In accordance with experimental data?**
data anaerobic	↗	not measured	↘	↘	↘	↘	↗	
k_1 ↗	↗	↗	↗	↗	↗	↗	↗	no
k_1 ↘	↗	↗	↗	↘	↗	↘	↗	no
k_2 ↗	↗	↗	↗	↘	↗	↗	↗	no
k_2 ↘	↗	↗	↗	↗	↗	↘	↗	no
k_{4b} ↗	↗	↗	↗	↗	↘	↗	↗	no
k_{4b} ↘	↗	↗	↗	↗	↗	↗	↘	no
k_{5b} ↗	↗	↗	↘	↗	↗	↗	↗	no
k_{5b} ↘	↗	↗	↗	↗	↘	↗	↘	no
k_7 ↗	↗	↗	↗	↗	↗	↗	↗	no
k_7 ↘	↗	↗	↘	↗	↘	↗	↘	no
k_8 ↗	↗	↗	↗	↗	↗	↗	↗	no
k_8 ↘	↗	↘	↗	↗	↗	↗	↗	no
k_9 ↗	↗	↘	↗	↗	↗	↗	↗	no
k_9 ↘	↗	↗	↗	↗	↗	↗	↗	no
k_{10} ↗	↗	↗	↗	↗	↗	↗	↘	no
k_{10} ↘	↗	↗	↗	↗	↗	↗	↗	no
k_{11} ↗	↗	↗	↗	↗	↗	↘	↗	no
k_{11} ↘	↗	↗	↗	↗	↗	↗	↗	no

Supplementary Table 4: Results obtained by decreasing k_1 and changing a second parameter in the hypothetical network in Figure 9, when the pathway acts as two branches (fermentation). The scenarios with qualitative behavior most similar to the experimental data are indicated in red. Abbreviations: see Figure 9 of the main text.

	PYR **A**	**ETH** **B**	**MAL** **OAA** **C**	**CIT** **ISOCIT** **D**	**FUM** **E**	**OGL** **F**	**SUC** **G**	**In accordance with experimental data?**
data anaerobic	↗	not measured	↘	↘	↘	↘	↗	
k_1 ↘, k_2 ↗	↗	↗	↗	↘	↗	↗	↗	no
k_1 ↘, k_2 ↘	↗	↗	↗	↗	↗	↘	↗	no
k_1 ↘, k_{4b} ↗	↗	↗	↗	↘	↘	↘	↗	no
k_1 ↘, k_{4b} ↘	↗	↗	↗	↘	↗	↘	↘	no
k_1 ↘, k_{5b} ↗	↗	↗	↘	↘	↗	↘	↗	no
k_1 ↘, k_{5b} ↘	↗	↗	↗	↘	↘	↘	↘	no
k_1 ↘, k_7 ↗	↗	↗	↗	↘	↗	↘	↗	no
k_1 ↘, k_7 ↘	↗	↗	↘	↘	↗	↗	↗	no
k_1 ↘, k_8 ↗	↗	↗	↗	↘	↗	↘	↗	no
k_1 ↘, k_8 ↘	↗	↗	↗	↗	↗	↗	↗	no
k_1 ↘, k_9 ↗	↗	↘	↗	↘	↗	↘	↗	no
k_1 ↘, k_9 ↘	↗	↗	↗	↘	↗	↘	↗	no
k_1 ↘, k_{10} ↗	↗	↗	↗	↘	↗	↘	↘	no
k_1 ↘, k_{10} ↘	↗	↗	↗	↘	↗	↘	↗	no
k_1 ↘, k_{11} ↗	↗	↗	↗	↘	↗	↘	↗	no
k_1 ↘, k_{11} ↘	↗	↗	↗	↘	↗	↗	↗	no

Supplementary Table 5: Results obtained by decreasing k_1, increasing k_{4b} or k_{5b} and changing a third parameter in the hypothetical network in Figure 9, when the pathway acts as two branches (fermentation). Results in accordance with the experimental data are indicated in red. Abbreviations: see Figure 9 of the main text.

	PYR **A**	**ETH** **B**	**MAL** **OAA** **C**	**CIT** **ISOCIT** **D**	**FUM** **E**	**OGL** **F**	**SUC** **G**	**In accordance with experimental data?**
data anaerobic	↗	not measured	↘	↘	↘	↘	↗	
k_1 ↘, k_{4b} ↗, k_2 ↗	↗	↗	↗	↘	↘	↗	↗	no
k_1 ↘, k_{4b} ↗, k_2 ↘	↗	↗	↗	↗	↘	↘	↗	no
k_1 ↘, k_{4b} ↗, k_{5b} ↗	↗	↗	↘	↘	↘	↘	↗	yes
k_1 ↘, k_{4b} ↗, k_{5b} ↘	↗	↗	↗	↘	↘	↘	↗	no
k_1 ↘, k_{4b} ↗, k_7 ↗	↗	↗	↗	↘	↘	↘	↗	no
k_1 ↘, k_{4b} ↗, k_7 ↘	↗	↗	↘	↘	↘	↘	↗	yes
k_1 ↘, k_{4b} ↗, k_8 ↗	↗	↗	↗	↘	↘	↘	↗	no
k_1 ↘, k_{4b} ↗, k_8 ↘	↗	↘	↗	↘	↘	↘	↗	no
k_1 ↘, k_{4b} ↗, k_9 ↗	↗	↘	↗	↘	↘	↘	↗	no
k_1 ↘, k_{4b} ↗, k_9 ↘	↗	↗	↗	↘	↘	↘	↗	no
k_1 ↘, k_{4b} ↗, k_{10} ↗	↗	↗	↗	↘	↘	↘	↘	no
k_1 ↘, k_{4b} ↗, k_{10} ↘	↗	↗	↗	↘	↘	↘	↗	no
k_1 ↘, k_{4b} ↗, k_{11} ↗	↗	↗	↗	↘	↘	↘	↗	no
k_1 ↘, k_{4b} ↗, k_{11} ↘	↗	↗	↗	↘	↘	↗	↗	no
k_1 ↘, k_{5b} ↗, k_2 ↗	↗	↗	↘	↘	↗	↗	↗	no
k_1 ↘, k_{5b} ↗, k_2 ↘	↗	↗	↘	↗	↗	↘	↗	no
k_1 ↘, k_{5b} ↗, k_{4b} ↘	↗	↗	↘	↘	↗	↘	↘	no
k_1 ↘, k_{5b} ↗, k_7 ↗	↗	↗	↗	↘	↗	↘	↗	no
k_1 ↘, k_{5b} ↗, k_7 ↘	↗	↗	↘	↘	↗	↘	↗	no
k_1 ↘, k_{5b} ↗, k_8 ↗	↗	↗	↘	↘	↗	↘	↗	no
k_1 ↘, k_{5b} ↗, k_8 ↘	↗	↘	↘	↘	↗	↘	↗	no
k_1 ↘, k_{5b} ↗, k_9 ↗	↗	↘	↘	↘	↗	↘	↗	no
k_1 ↘, k_{5b} ↗, k_9 ↘	↗	↗	↘	↘	↗	↘	↗	no
k_1 ↘, k_{5b} ↗, k_{10} ↗	↗	↗	↘	↘	↗	↘	↘	no
k_1 ↘, k_{5b} ↗, k_{10} ↘	↗	↗	↘	↘	↗	↘	↗	no
k_1 ↘, k_{5b} ↗, k_{11} ↗	↗	↗	↘	↘	↗	↘	↗	no
k_1 ↘, k_{5b} ↗, k_{11} ↗	↗	↗	↘	↘	↗	↗	↗	no

2 Validation of the results

2.1 Simulation models of glycolysis

Models for glycolysis in *Saccharomyces cerevisiae* from the literature were used. Aerobic glucose pulse experiments were simulated with the glucose pulse model (aerobic, glucose-limited chemostat) developed by van Eunen [7]. To simulate anaerobic pulse experiments, the parameters in the aerobic model were adapted according to Daran-Lapujade *et al.* [1]. An overview of the parameters used in this study is given in Supplementary Table 6. The differential equations are described in van Eunen [7]. The models simulate a sustained glucose concentration after the pulse. Because of this, they mimic the trend of the experiments (transient increase of glucose) well in only a small time interval after the pulse [7]. Therefore, 0-1 minute was chosen as the window of observation for the simulated data. The rates to the branches are assumed to be constant in the models. The absolute levels of some metabolites are not well described by the model (for details, see [7]) but the trends obtained largely agree with the trends observed in the data.

For each experiment, 11 equidistantly sampled time points, with sampling frequency 0.1 minutes, were generated. Noise drawn from a random normal distribution, with zero mean and a standard deviation of 0.15, was added to the noiseless data. For each environmental condition, 10 replicates were simulated.

Matlab's ordinary differential equation solver ode15s [5] was used for calculating concentration values over time and determining steady state concentrations.

Supplementary Table 6: Model parameters in the glucose pulse model. Values for aerobic conditions were taken from [7].V_{max} values for anaerobic conditions were calculated from $V_{max,aerobic}/V_{max,anaerobic}$ ratios reported in [1].

parameter	value (aerobic)	value (anaerobic)	parameter	value (aerobic)	value (anaerobic)
$C_{GLCex,steady-state}$	0.2	0.2	$C_{ATP,steady-state}$	3	3
$C_{ATP,after_pulse}$	1.5	1.5	C_{ETOH}	0.37	30.99 [6]
$V_{max,GLT}$	160	220 [7]	$K_{m,GLT,GLCex}$	1	0.9 [2]
$K_{m,GLT,GLCin}$	1	0.9 [2]	$K_{eq,GLT}$	1	1
$V_{max,HK}$	213	426	$K_{m,HK,GLCin}$	0.08	0.08
$K_{m,HK,G6P}$	30	30	$K_{I,HK,T6P}$	0.04	0.04
$K_{m,HK,ATP}$	0.15	0.15	$K_{m,HK,ADP}$	0.23	0.23
$K_{eq,HK}$	3800	3800	$V_{max,PGI}$	787	1574
$K_{m,PGI,G6P}$	1.4	1.4	$K_{m,PGI,F6P}$	0.3	0.3
$K_{eq,PGI}$	0.314	0.314	K_{TRE1}	0	7.5512
K_{TRE2}	0	0	$V_{max,PFK}$	213	319.5

gR	5.12	5.12	L_0	0.66	0.66
$K_{m,PFK,F6P}$	0.1	0.1	$K_{m,PFK,ATP}$	0.71	0.71
$C_{PFK,ATP}$	3	3	$K_{PFK,AMP}$	0.0995	0.0995
$C_{PFK,AMP}$	0.0845	0.0845	$K_{i,PFK,ATP}$	0.65	0.65
$C_{i,PFK,ATP}$	100	100	$K_{PFK,F26BP}$	0.000682	0.000682
$C_{PFK,F26BP}$	0.0174	0.0174	$K_{PFK,F16BP}$	0.111	0.111
$C_{PFK,F16BP}$	0.397	0.397	$K_{eq,TPI}$	0.045	0.045
$V_{max,ALD}$	310	206.67	$K_{m,ALD,F16P}$	0.3	0.3
$K_{m,ALD,GAP}$	2	2	$K_{m,ALD,DHAP}$	2.4	2.4
$K_{m,ALD,GAPi}$	10	10	$K_{eq,ALD}$	0.069	0.069
K_{GLY}	10	10	$V_{max,GAPDHf}$	1300	2600
$V_{max,GAPDHr}$	853	853	$K_{m,GAPDH,GAP}$	0.21	0.21
$K_{m,GAPDH,BPG}$	0.036	0.036	$K_{m,GAPDH,NAD}$	2.8	2.8
$K_{m,GAPDH,NADH}$	0.06	0.06	C_{GAPDH}	1	1
$NADt$	1.59	1.59	$V_{max,PGK}$	2512	5024
$K_{m,PGK,BPG}$	0.003	0.003	$K_{m,PGK,3PG}$	0.53	0.53
$K_{m,PGK,ADP}$	0.2	0.2	$K_{m,PGK,ATP}$	0.3	0.3
$K_{eq,PGK}$	3200	3200	$V_{max,PGM}$	856	1712
$K_{m,PGM,3PG}$	1.2	1.2	$K_{m,PGM,2PG}$	0.08	0.08
$K_{eq,PGM}$	0.19	0.19	$V_{max,ENO}$	357	535.5
$K_{m,ENO,2PG}$	0.04	0.04	$K_{m,ENO,PEP}$	0.5	0.5
$K_{eq,ENO}$	6.7	6.7	$V_{max,PYK}$	820	1640
$K_{m,PYK,PEP}$	0.19	0.19	$K_{m,PYK,ADP}$	0.3	0.3
$K_{m,PYK,ATP}$	9.3	9.3	n_{10}	4	4
L_{10}	60000	60000	$K_{m,PYK,F16P}$	0.2	0.2
$V_{max,PDC}$	395	790	$K_{m,PDC,PYR}$	6.36	6.36
NH_{PDC}	1.9	1.9	$V_{max,ADH}$	932	372.80
$K_{m,ADH,ACALD}$	1.11	1.11	$K_{m,ADH,ETOH}$	17	17
$K_{m,ADH,NADH}$	0.11	0.11	$K_{m,ADH,NAD}$	0.17	0.17
$K_{i,ADH,ACALD}$	1.1	1.1	$K_{i,ADH,ETOH}$	90	90
$K_{i,ADH,NADH}$	0.031	0.031	$K_{i,ADH,NAD}$	0.92	0.92
$K_{eq,ADH}$	$6.9 * 10^{-5}$	$6.9 * 10^{-5}$	K_{SUC}	0.9	0.9
K_{ACE}	0.5	730	ADP	1	1
AMP	0.3	0.3	CO_2	1	1
$T6P$	0.2	2.2	$TREH$	2	2
$F26BP$	0.014	0.014	GLY	10	10
ACE	10	10			

2.2 Correspondence of the results of the simulated and the experimental data

The sustained correlations between G6P and F6P and between 3PG and PEP, as well as the reversed correlation between FBP and 3PG could be observed for both simulated and experimental data (see Supplementary Table 7). The added noise levels had no effect on the sign of the correlation, but in some cases decreases the value of the Pearson correlation coefficient.

Supplementary Table 7: Comparison of the results of the correlation analysis for the simulation studies and the experimental data. Number of replicates between brackets.

metabolites		**aerobic**			**anaerobic**		
		2.5 mM GLUC			3 mM GLUC		
		exp (3)	sim (noise-less) (1)	sim (15% noise) (10)	exp (1)	sim (noise-less) (1)	sim (15% noise) (10)
G6P	F6P	+++	+++	+++	+++	+++	++
FBP	3PG	- - -	- - -	- - -	++	+++	+
3PG	PEP	+++	+++	+++	++	+++	+

Categories: +++, high positive correlation; ++, moderate positive correlation; +, low positive correlation; 0, zero correlation; -, low negative correlation; - -, moderate negative correlation; - - -, high negative correlation.

Abbreviations: GLUC, glucose; G6P, glucose-6-phosphate; F6P, fructose-6-phosphate; FBP, fructose-1,6-bisphosphate; 3PG, 3-phosphoglycerate; PEP, phosphoenolpyruvate; PYR, pyruvate; exp, experiment; sim, simulation.

2.3 Relation between higher reaction rates in lower glycolysis and feed-forward activation of pyruvate kinase by FBP

The higher reaction rates in the lower part of glycolysis, caused by a glucose pulse under aerobic conditions, can be explained by the feed-forward activation of pyruvate kinase by FBP [3] (see Figure 11). In the presence of oxygen, a glucose pulse causes a large increase in FBP (FBP increases a few orders of magnitude during the first 30 seconds after the pulse) [4]. This causes a large increase in pyruvate kinase activity, which in turn causes a large increase in reaction rates in the lower part of glycolysis. If this allosteric effect of FBP on pyruvate kinase is removed from the equation of pyruvate kinase in the model, the correlation between FBP and 3PG becomes positive (see Supplementary Figure 1), which confirms our explanation. Under anaerobic conditions, the FBP level is already high before the pulse. The FBP concentration also increases, but is in the same order of magnitude as before the pulse [6]. Therefore, there is no large increase in pyruvate kinase activity and as a consequence no large increase in the reaction rates in the lower part of glycolysis and the correlation between FBP and 3PG is positive. So this implies that the correlation inversion can be explained solely as the result of initial conditions and the presence of the feedforward loop.

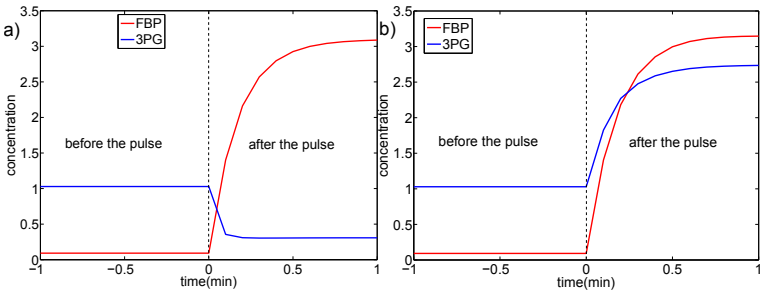

Supplementary Figure 1: Concentration profiles of FBP and 3PG a) if FBP has an allosteric effect on pyruvate kinase b) if FBP has no allosteric effect on pyruvate kinase.

3 Scenarios independent of the order of the mass-action kinetics

3.1 Example: second order reaction kinetics

Consider again the hypothetical network of Figure 6 of the main article, but assume that the reactions from A to B and from C to D are second order ($2A \rightarrow B$ and $2C \rightarrow D$). The mass balances for the metabolites are

$$\begin{aligned}
\frac{d[A]}{dt} &= in - k_1 * [A]^2 \\
\frac{d[B]}{dt} &= k_1 * [A]^2 - k_2 * [B] \\
\frac{d[C]}{dt} &= k_2 * [B] - k_3 * [C] - k_4 * [C]^2 \\
\frac{d[D]}{dt} &= k_4 * [C]^2 - k_6 * [D] \\
\frac{d[E]}{dt} &= k_3 * [C] - k_5 * [E]
\end{aligned}$$

where $in = 1$ and $k_1 = k_2 = k_3 = k_4 = k_5 = k_6 = 1$.

The steady state of this system is $[A] = [B] = 1$, $[C] = [E] = 0.6180$ and $[D] = 0.3820$. A pulse is simulated by changing the inflow to $in = 2$. The response shows a positive correlation between B and D (see Supplementary Figure 2). An increase in B and a decrease in D as an initial response to the pulse is only observed in the following situations:

- a smaller rate of the reaction converting B to C (a lower value for k_2, see Supplementary Figure 3a);
- a larger rate of the reaction converting C to E in the branch (a higher value for k_3, see Supplementary Figure 3b);
- a smaller rate of the reaction converting C to D (a lower value for k_4, see Supplementary Figure 3c);
- a larger rate of the reaction that further metabolizes D (a higher value for k_6, see Supplementary Figure 3d);

The inferred correlation scenarios are the same as for the first order reaction network.

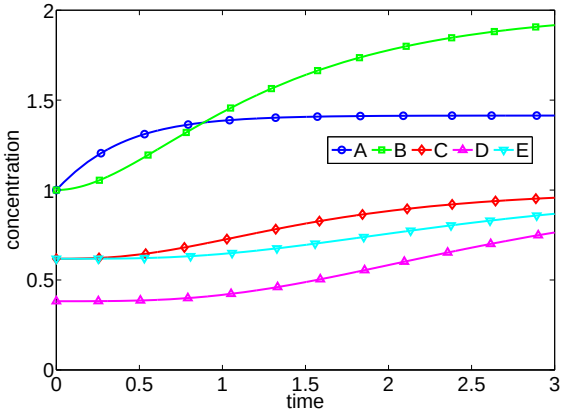

Supplementary Figure 2: Response of the metabolites in the *in silico* hypothetical network model of Figure 6 to an increase in the inflow in the second order reactions case. The numbers on the axes are in arbitrary units.

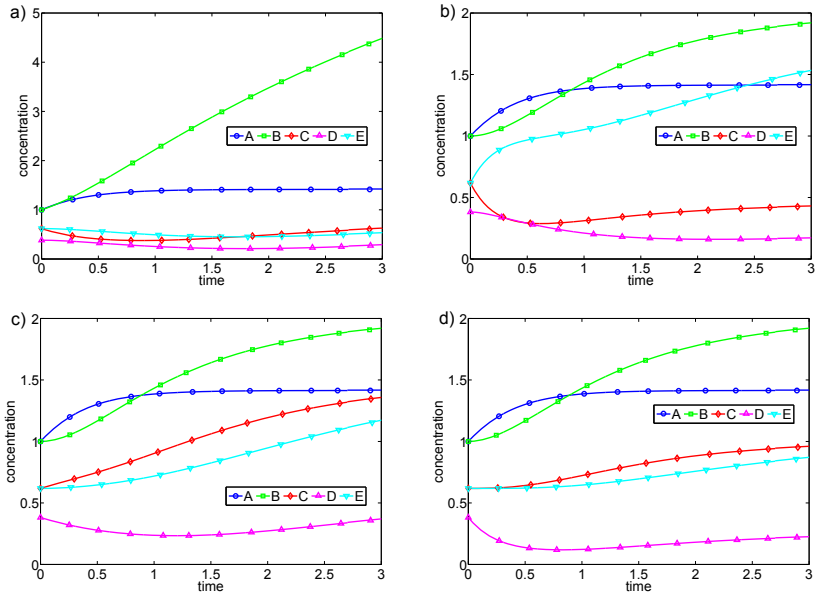

Supplementary Figure 3: Changes in the parameters that lead to the emergence of a negative correlation between B and D in the second order reactions case: a) a lower value for k_2 ; b) a higher value for k_3; c) a lower value for k_4; d) a higher value for k_6. The numbers on the axes are in arbitrary units.

3.2 General proof

Let's assume a hypothetical network with n metabolites $X_1, \cdots, X_n$ with only reactions with one substrate and one product (like the simplified models in the main manuscript). Assume that for $i, j \in \{1, \cdots, n\}$:
$k_{ij} > 0$ is the reaction rate and n_{ij} the order of the reaction $X_i \rightarrow X_j$;
$k_{ij} = n_{ij} = 0$ if there is no reaction $X_i \rightarrow X_j$;
$k_{ij(steady\ state)} > 0$ is the steady state reaction rate of the reaction $X_i \rightarrow X_j$;
$k_{ij(steady\ state)} = 0$ if there is no reaction $X_i \rightarrow X_j$ under steady state.
The mass balances for this hypothetical network are ($i = 1, \cdots, n$):

$$\frac{dX_i}{dt} = \underbrace{\sum_{j=1}^{n} k_{ji} X_j^{n_{ji}}}_{incoming\ reactions} - \underbrace{\sum_{j=1}^{n} k_{ij} X_i^{n_{ij}}}_{outgoing\ reactions}$$

Suppose there is a reaction $X_p \rightarrow X_q$ with reaction rate k_{pq}. Under steady state, the mass balances for X_p and X_q are:
$\frac{dX_p}{dt} = \sum_{j=1}^{n} k_{jp(steady\ state)} X_j^{n_{jp}} - \sum_{j=1}^{n} k_{pj(steady\ state)} X_i^{n_{pj}} = 0$
$\frac{dX_q}{dt} = \sum_{j=1}^{n} k_{jq(steady\ state)} X_j^{n_{jq}} - \sum_{j=1}^{n} k_{qj(steady\ state)} X_i^{n_{qj}} = 0$
If k_{pq} increases after a perturbation, then:
$\frac{dX_p}{dt} = \sum_{j=1}^{n} k_{jp(steady\ state)} X_j^{n_{jp}} - \sum_{j=1, j\neq q}^{n} k_{pj(steady\ state)} X_i^{n_{pj}} - \underbrace{k_{pq} X_p^{n_{pq}}}_{>than\ under\ steady\ state} < 0$
which means that X_p decreases as initial response to the pulse, regardless of the order of the reactions.
$\frac{dX_q}{dt} = \underbrace{k_{pq} X_j^{pq}}_{>than\ under\ steady\ state} + \sum_{j=1, j\neq p}^{n} k_{jq(steady\ state)} X_j^{n_{jq}} - \sum_{j=1}^{n} k_{qj(steady\ state)} X_i^{n_{qj}} > 0$
which means that X_q increases as initial response to the pulse, regardless of the order of the reactions.
In the same way it can be proved that when k_{pq} decreases after a perturbation, then X_p increases en X_q decreases as initial response to the pulse, regardless of the order of the reactions. It can be concluded that the qualitative behavior of the graphs after the pulse is independent of the order of the mass-action kinetics.

4 Regulation scenarios TCA cycle

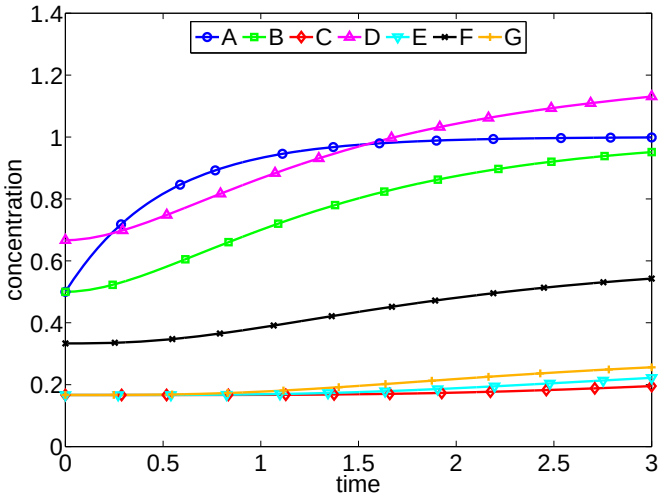

Supplementary Figure 4: Response of the metabolites in the *in silico* hypothetical network model of Figure 9 to an increase in the inflow when the pathway acts as a cycle before the pulse and there are no changes in the distribution of the reaction rates. The numbers on the axes are in arbitrary units.

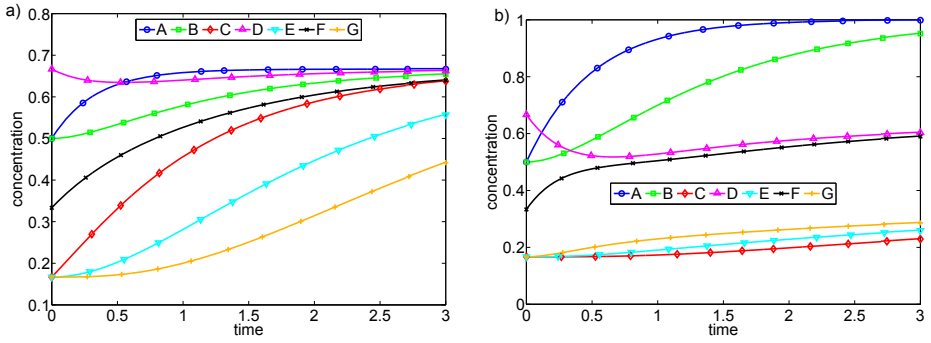

Supplementary Figure 5: Changes in the parameters that lead to a decrease in D and an increase of A, C, E, G and F when the pathway acts as a cycle before the pulse: a) TCA cycle acts as two branches; b) higher value of k_2 after the pulse. The numbers on the axes are in arbitrary units.

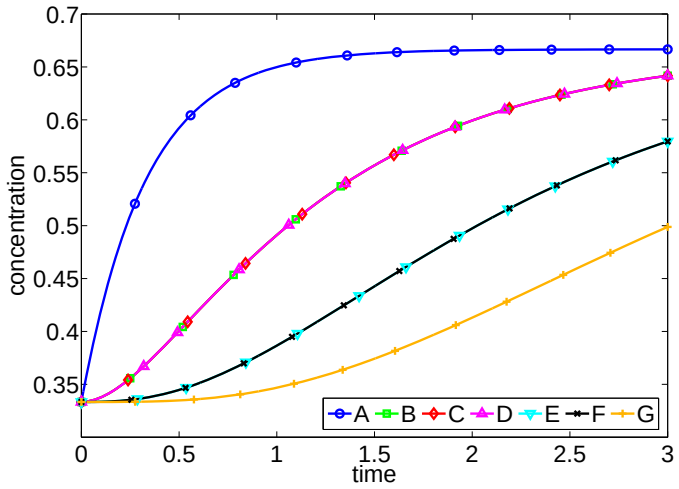

Supplementary Figure 6: Response of the metabolites in the *in silico* hypothetical network model of Figure 9 to an increase in the inflow when the pathway acts as two branches before the pulse and there are no changes in the distribution of the reaction rates. The numbers on the axes are in arbitrary units.

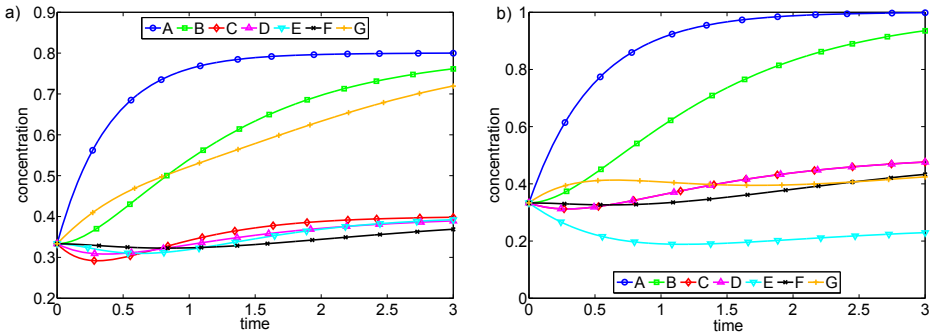

Supplementary Figure 7: Changes in the parameters that lead to an increase in A and G and a decrease in C, D, E and F when the pathway acts as two branches before the pulse: a) a lower value for k_1 and higher values for k_{4b} and k_{5b} after the pulse; b) lower values for k_1 and k_7 and a higher value for k_{4b} after the pulse. The numbers on the axes are in arbitrary units.

5 Experimental data

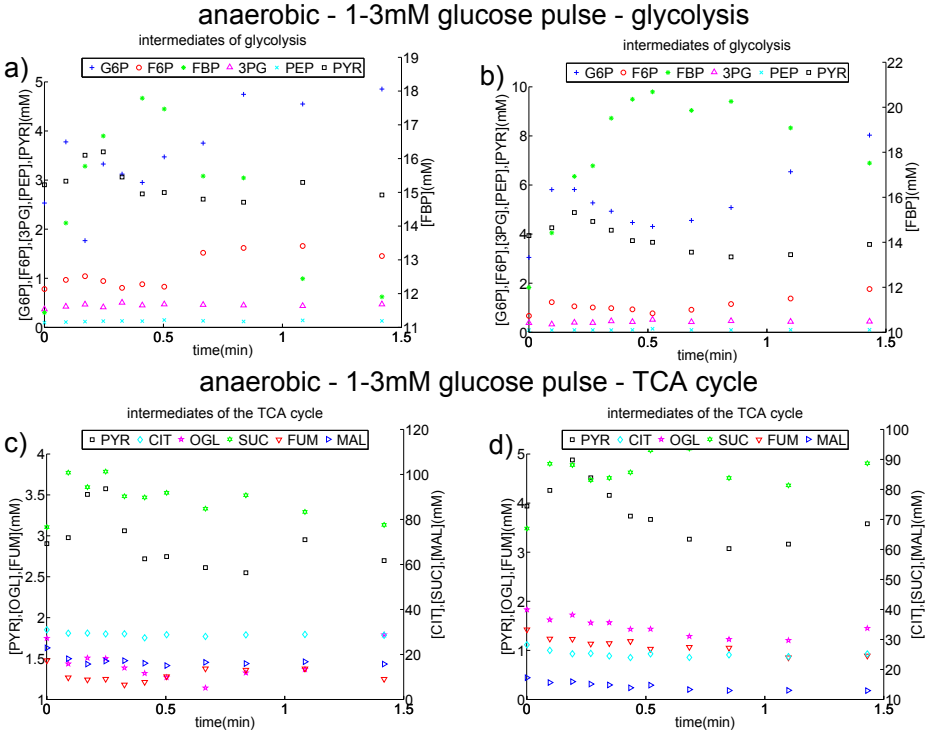

Supplementary Figure 8: Experimental data: response of glycolysis (a-b) and the TCA cycle (c-d) to a 1-3 mM glucose pulse under anaerobic conditions. Abbreviations: see main text.

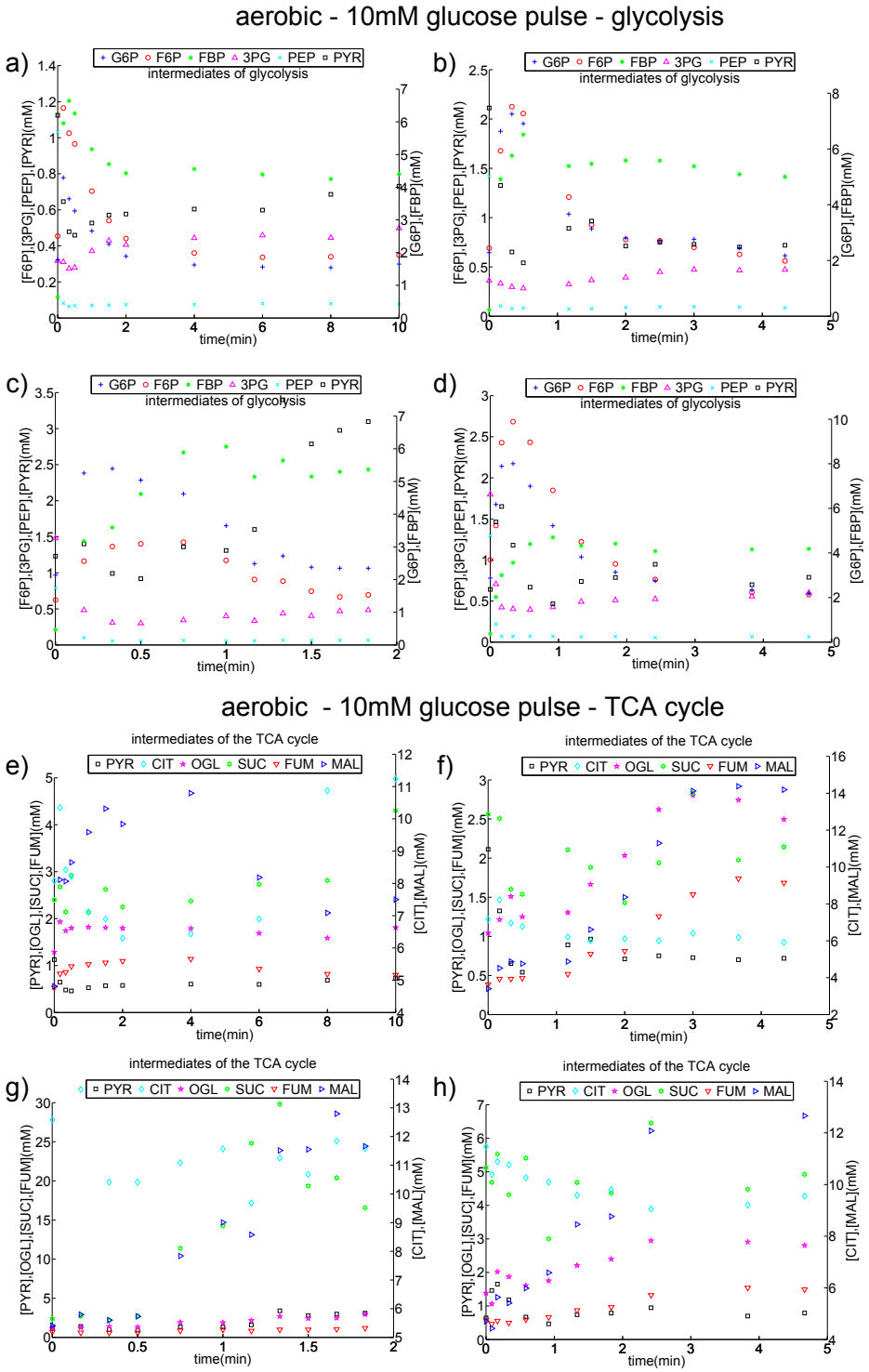

Supplementary Figure 9: Experimental data: response of glycolysis (a-d) and the TCA cycle (e-h) to a 10 mM glucose pulse under aerobic conditions. Abbreviations: see main text.

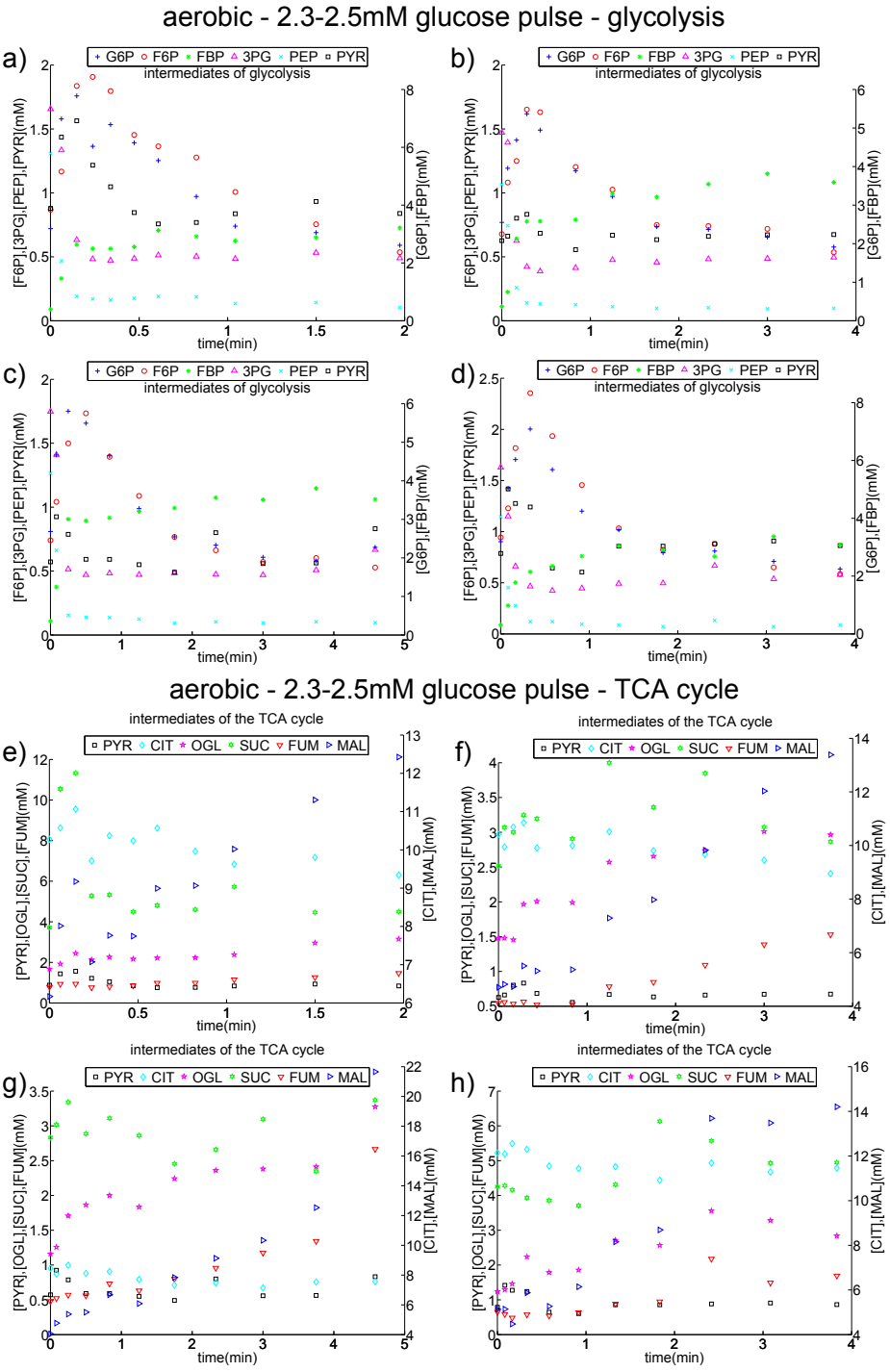

Supplementary Figure 10: Experimental data: response of glycolysis (a-d) and the TCA cycle (e-h) to a 2.3-2.5 mM glucose pulse under aerobic conditions. Abbreviations: see main text.

Acknowledgements This project was financed by the Netherlands Metabolomics Centre (NMC) which is part of the Netherlands Genomics Initiative /Netherlands Organisation for Scientific Research. Karen van Eunen and Barbara Bakker (University Medical Center Groningen) are gratefully acknowledged for providing us with the simulation models.

References

[1] P. Daran-Lapujade, S. Rossell, W. M. van Gulik, M. A. Luttik, M. J. de Groot, M. Slijper, A. J. Heck, J. M. Daran, J. H. de Winde, H. V. Westerhoff, J. T. Pronk, and B. M. Bakker. The fluxes through glycolytic enzymes in saccharomyces cerevisiae are predominantly regulated at posttranscriptional levels. *Proc Natl Acad Sci U S A*, 104(40):15753–8, 2007.

[2] J.A. Diderich, M. Schepper, P. van Hoek, M. A. H. Luttik, J. P. van Dijken, J. T. Pronk, P. Klaassen, H. F. M. Boelens, M. J. Teixeira de Mattos, K. van Dam, and A. L. Kruckeberg. Glucose uptake kinetics and transcription of hxt genes in chemostat cultures of saccharomyces cerevisiae. *Journal of Biological Chemistry*, 274(22):15350–15359, 1999.

[3] M.S. Jurica, A. Mesecar, P.J. Heath, S. Wuxian, T. Nowak, and B.L. Stoddard. The allosteric regulation of pyruvate kinase by fructose-1,6-bisphosphate. *Structure*, 6(2):195–210, 1998.

[4] T. Kamminga. Short-term dynamics of glycolysis in saccharomyces cerevisiae expressing arginine kinase. Master's thesis, Department of Biotechnology, Delft University of Technology, February, 2007.

[5] MATLAB®. Version 7.11.0.(r2010b), microsoft windows xp version 5.1., copyright©, 1984-2010,The Mathworks Inc.

[6] I. E. Nikerel, A. B. Canelas, S.J. Jol, P. J. T. Verheijen, and J. J. Heijnen. Construction of kinetic models for metabolic reaction networks: Lessons learned in analysing short-tern stimulus response data. *Mathematical and Computer Modelling of Dynamical Systems*, 17(3):243–260, 2011.

[7] K. van Eunen. *The multifarious and dynamic regulation of the living cell.* PhD thesis, Free University of Amsterdam, 2010.